I&EC research
Industrial & Engineering Chemistry Research

pubs.acs.org/IECR

Article

Palm Oil Valorization through the Oxidative Cleavage of Unsaturated Fatty Acids with Ru-Carbon Catalysts

Sebastián Gámez,* Ernesto de la Torre, and Eric M. Gaigneaux

Cite This: https://doi.org/10.1021/acs.iecr.2c04498

Read Online

ACCESS | Metrics & More | Article Recommendations | Supporting Information

ABSTRACT: Palm oil valorization for the production of azelaic acid, highly demanded for the treatment of skin cancer, was performed through the oxidative cleavage of unsaturated fatty acids. In this reaction, olefinic bonds are broken to yield carboxylic and dicarboxylic acids. To do so, carbon black and carbon micrometric particles were functionalized with polydopamine to form complexes with Ru. These Ru-carbon catalysts were fully characterized before catalytic tests, where triglycerides within palm oil were transformed into fatty acid methyl esters first and then incorporated in our catalytic system formed by H_2O/MeCN/AcOEt. After adding $NaIO_4$ and *N*-methylmorpholine *N*-oxide (oxidizing agents), our Ru-carbon catalysts reached a complete >99% conversion in 5 h of reaction at room temperature with yields of azelaic acid around 85%. Although Ru species were found in the liquid phase during the reaction, the solid catalysts managed to recover them to keep the same catalytic activity for five recycling tests. Therefore, our Ru-carbon catalysts open a novel route for the production of a high-value-added product with medicinal applications from a cheap feedstock such as palm oil.

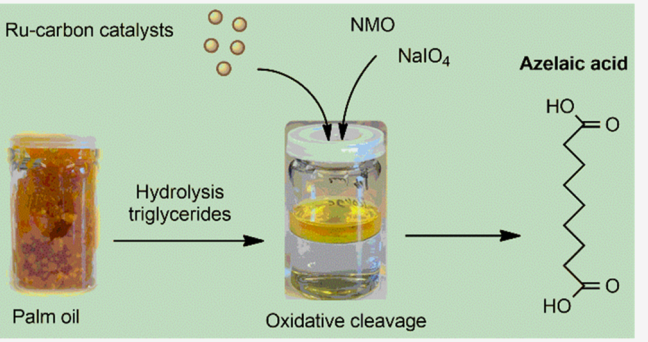

1. INTRODUCTION

Palm oil extracted from the fruit known as *Elaies guineensis* is one of the most important vegetable oils because of its abundance, low price, and high content of unsaturated fatty acids (UFAs).[1,2] This reddish brown oil, which presents a semisolid consistency at ambient temperature, is produced in tropical areas of Africa and Latin America.[3] Palm oil is constituted of triglycerides with saturated (SFAs) and unsaturated fatty acids as well as minor components such as carotenoids. This oil is widely employed as a raw material for the preparation of several food products like cooking oils, margarine, baking fats, or confectionery baking fats.[4] However, in the last two decades, different oils and fats, like palm oil, have been used in nonfood applications for the synthesis of value-added products.[5,6] Recently, UFAs within several oils have been employed as a novel source of chemical base materials for various industries (e.g., plasticizers, polymers, biodiesel).[7,8] Among the most interesting applications, there is the production of azelaic acid (AA) by means of the oxidative cleavage reaction.[9] AA is a dicarboxylic acid (C9), which is normally extracted from cultures of Pityrosporum ovale fungus. It is commonly used as the main ingredient for creams and other cosmetics.[10] Moreover, it is employed to cure cutaneous malignant melanoma since AA can destroy abnormal melanocytes.[10] Usually, oxidative cleavage of pure UFAs is carried out by ozonolysis, which is also a highly energy-demanding process.[11] Another option is the use of homogeneous catalysts, which employ transition metals such as Ru, Os, or W along with harmful oxidizing agents.[6] Most of the works published so far are related to homogenous catalysts, which present great results in terms of conversion and yield, but they cannot be recovered after the reaction ends.[12−14]

On the other hand, few heterogeneous catalysts have been developed due to the poor results obtained in this matter. The difficulty of anchoring high oxidation transition metals on suitable supports, the loss of active sites by leaching, and steric hindrances due to the size of the UFAs are just some drawbacks that heterogeneous catalysis must deal with in the oxidative cleavage of UFAs.[15−17] It is important to note that oleic (18:1 n-9) and linoleic (18:2 n-9,12) acids are the most abundant UFAs within palm oil and they can both be used for the production of azelaic acid. In addition, there are a few examples in the literature about the oxidative cleavage of real vegetable oil.[17,18] Therefore, we propose a new heterogeneous catalyst that addresses the oxidative cleavage of UFAs contained inside palm oil using carbon black (CB) and carbon spheres (CS) as main supports. CB possesses several functional groups (i.e., phenols, lactones), which can be introduced on its

Received: December 13, 2022
Revised: March 8, 2023
Accepted: March 8, 2023

surface through oxidation treatments. Its low cost and accessibility make CB a suitable support for heterogeneous catalyst fabrication.[19,20] CS, on the other hand, can be synthesized by heating an aqueous solution with a carbon precursor (e.g., fructose, glucose) under autogenous pressure, a process known as hydrothermal carbonization. This green method can produce well-distributed carbon spheres bearing several oxygenated functionalities without any additional hazardous treatment.[21−23]

In our recent publication, Ru complexes on oxidized carbon black (CBO) previously functionalized with polydopamine (PDA) were used for the oxidative cleavage of pure oleic acid efficiently.[24] PDA is an organic polymer that contains amine and catechol groups that can complex transition metals like Ru.[25−27] In our catalytic system, the functional groups of PDA release Ru ions in the reaction medium, where they are oxidized by $NaIO_4$ into $Ru^{VIII}O_4$ to cleave olefinic bonds of UFAs through a pericyclic [3 + 2] reaction. When all UFAs are transformed into carboxylic acids (products from the oxidative cleavage of UFAs), the functional groups of PDA recover Ru species, allowing us to reuse the catalyst multiple times.[24] In fact, PDA functions as a redox ligand yielding different catechol, semi-quinone radicals, and quinone groups that may reduce Ru species and complex them.[28−30] Based on this success, we here report the functionalization of CBO and CS with PDA and Ru toward the oxidative cleavage of UFAs from palm oil to assess the feasibility of performing this reaction on a complex mixture of fatty acids (FAs) that a real oil represents. Finally, *N*-methylmorpholine *N*-oxide (NMO) was also incorporated into our catalytic system to assess the possibility of replacing $NaIO_4$ or, at least, reducing the consumption of this oxidizing agent using a greener one. It is known that NMO can reoxidize Os^{VI} to Os^{VIII} species during the dihydroxylation of olefins.[31,32] Therefore, the possibility of applying this oxidizing agent for the regeneration of $Ru^{VIII}O_4$ was explored.

2. EXPERIMENTAL PROCEDURES

2.1. Preparation of Carbon Supports. First, 10 g of CB (Degussa Printex G) was introduced in a 5.0 M nitric acid (HNO_3 > 65% from Carl Roth) solution to be heated under reflux and magnetic stirring for 8 h at 90 °C. Then, CBO was recovered from the suspension by means of a Heraeus MultifugeX1R Centrifuge at 14 000 rpm (26 200*g*) for 40 min. CBO was washed with distilled H_2O at 80 °C until the pH of the solution attained a value of 6.5. Finally, CBO was dried in a furnace under an air atmosphere at 110 °C overnight. CS was produced by preparing a 0.2 M glucose (>98%, Carl Roth) aqueous solution, which was collocated inside a stainless-steel autoclave. Next, it was heated up to 180 °C under autogenous pressure for 24 h in a MEMMERT GmbH oven. The slurry obtained was washed thoroughly with distilled H_2O and ethanol. Afterward, calcined carbon particles (CCS) were produced after soft calcination of CS in a Vecstar furnace (air atmosphere) for 20 min at 420 °C.

2.2. Catalyst Preparation. First, PDA was deposited on both carbon supports (i.e., CBO and CCN). Consequently, 121 mg of tris(hydroxymethyl)aminomethane (>99.0%, TCI chemicals) was dissolved in 100 mL of distilled H_2O (10 mM). The latter was magnetically stirred under air atmosphere for 15 min and then 350 mg of dopamine hydrochloride (>98%, TCI chemicals) was added. The polymerization of DA took place when the clear solution turned light brown. Immediately, 1 g of either CBO or CCS was incorporated into the vessel and the mixture was stirred in the presence of air for 24 h. Next, the suspensions were centrifuged in a Heraeus MultifugeX1R Centrifuge at 14 000 rpm (26 200*g*) to retrieve the carbon supports with PDA on their surfaces (i.e., CBO-PDA and CCS-PDA). The functionalized solids were washed with distilled H_2O prior to drying under ambient air overnight at room temperature. As a reference material, pure PDA was synthesized as well, following the same procedure described but without a carbon support. For Ru impregnation, 500 mg of each functionalized support was introduced in 20 mL of distilled water and the suspension was submitted to ultrasound for 15 min. Then, 23 mg of $RuCl_3{\cdot}H_2O$ (99.9% PGM basis from Alfa Aesar) was introduced in 10 mL of distilled H_2O (10 mM). The Ru solution was incorporated into the ultrasound suspension to incorporate metal ions onto the carbon support (2 wt % Ru). The latter was magnetically stirred at room temperature for 24 h, and after that time, the carbon catalysts were retrieved from the solution by centrifugation. Finally, 25 mL of distilled H_2O was added three times to wash the Ru-carbon catalysts, and the solids were dried under an air atmosphere at room temperature overnight. The new carbon catalyst prepared with CBO as a support is called CBO-PDA-Ru(2%), while the one synthesized with CCS is entitled as CCS-PDA-Ru(2%).

2.3. Characterization. All carbon materials were characterized through electron microscopy (TEM) using an LEO 922 microscope with a LaB6 thermal cathode and an acceleration voltage of 200 kV. The average particle size was obtained after building a histogram of frequency distribution, taking into account around 20−25 particles of each sample. N_2 physisorption was also applied with Micromeritics Tristar 3000 equipment. For this purpose, samples of around 60 mg were degassed under vacuum (∼10.7 Pa) at 150 °C for 12 h. Isotherms were built by obtaining relative pressures (P/P_0) when samples were submitted to −196 °C. The specific surface area was calculated through the Brunauer−Emmet−Teller (BET) method considering P/P_0 between 0.05 and 0.30. In the case of microporous materials, the BET equation was applied at relative pressures ranging from 0.004 to 0.08.[33] The external surface area was determined through the *t*-plot procedure considering the linear portion of the slope P/P_0 between 0.3 and 0.8. Taking advantage of this method, the intercept of the *t*-plot (in mol/g) was used to determine the micropore volume using a density conversion factor of 34.54 cm^3/mol, while the total pore volume corresponded to the adsorbed volume at P/P_0 = 0.98.

The Barrett, Joyner, and Halenda method (BJH) was used to estimate the pore size distribution of meso- and macroporous materials employing P/P_0 from the desorption branch.[33] On the other hand, the Horvath−Kawazoe (HK) method was employed for pore size distribution determination in the case of microporous materials.[33] Thermogravimetric analysis (TGA) was also performed by putting ∼2 mg of each carbon sample inside Al_2O_3 crucibles of 70 μL of volume. Next, samples were heated from 50 to 900 °C (with a ramp 10 °C/min) in a Mettler Toledo TGA/SDTA851e Thermogravimetric Analyzer using a N_2 flow rate of 40 mL/min.

Carbon materials were also characterized through Fourier transform infrared spectroscopy (FTIR). Thus, 300 mg of KBr (>99%, Acros Organics) previously dried at 110 °C was thoroughly mixed with ∼15 mg of each carbon material. The solid mixtures were pressed up to 10 tons to prepare wafers

https://doi.org/10.1021/acs.iecr.2c04498
Ind. Eng. Chem. Res. XXXX, XXX, XXX−XXX

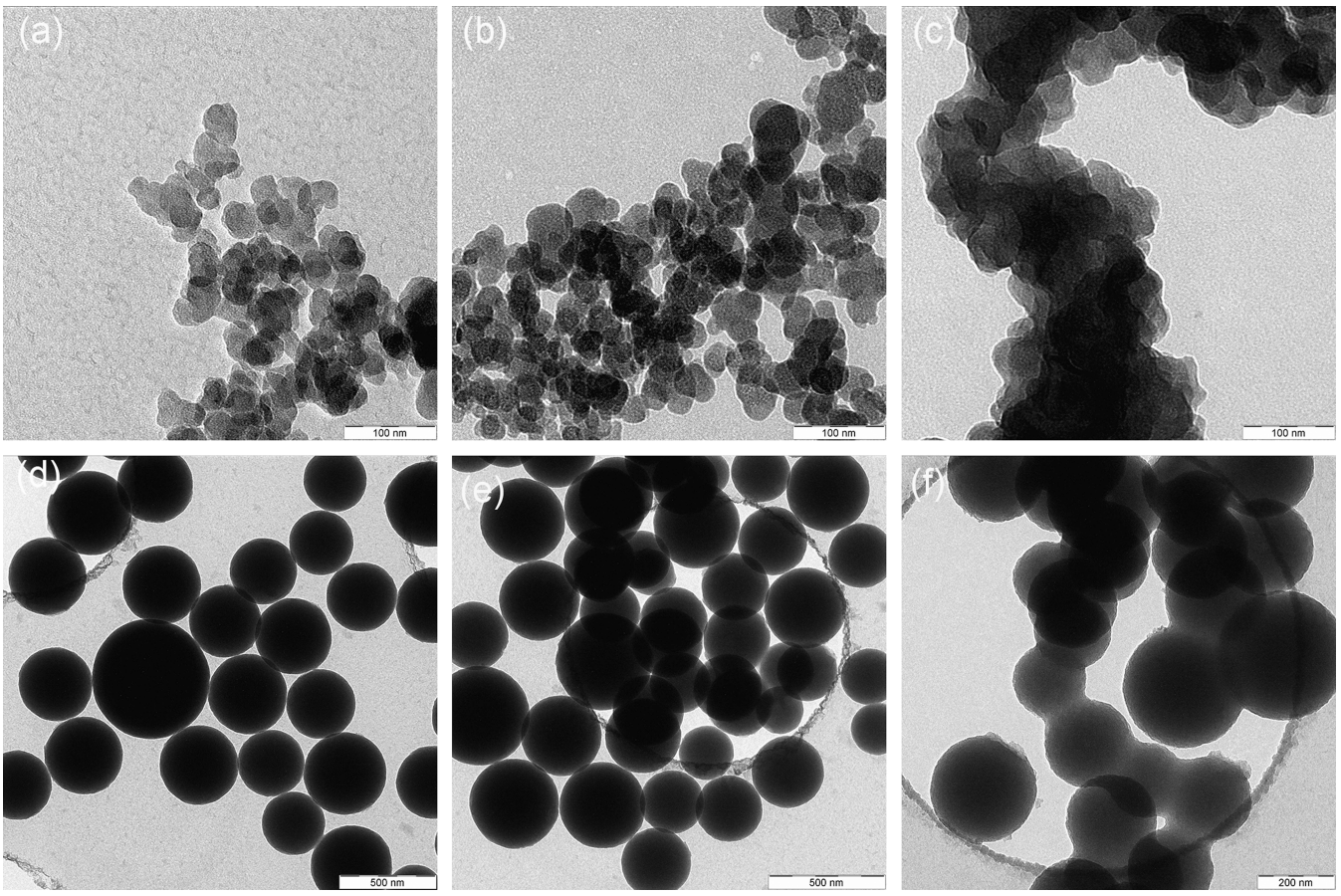

Figure 1. TEM photos of (a) CB; (b) CBO; (c) CBO-PDA; (d) CS; (e) CCS; and (f) CCS-PDA.

prior to analyses using a Bruker Equinox 55 FTIR spectrometer in transmission mode. Tests were conducted with 100 scans with a spectral window amid 4000 and 400 cm^{-1} (4 cm^{-1} of resolution) to record infrared spectra. Additionally, total acidity, along with the quantification of oxygen functionalities on carbon samples, was determined through Boehm's titration methodology and was applied to quantify oxygen groups following the procedure described elsewhere.[34,35] ICP-AES spectrophotometry analysis was conducted to measure Ru loading on the different carbon catalysts. For this purpose, around 100 mg of each carbon catalyst was collocated in a previously heated Vecstar furnace at 550 °C. Next, 1 g of Na_2O_2 and 1 g of NaOH were mixed along with the calcined carbon catalysts in an agate mortar. The solids were melted using a Bunsen burner and the product was allowed to cool down prior to dilution with 1000 mL of 10 v/v% HCl (37 v/v%, Carl Roth). The Ru content was measured in all liquid samples with an ICP 6500 Thermo Scientific Instrument.

X-ray photoelectron spectroscopy (XPS) tests were also conducted using an SX 100/206 photoelectron spectrometer equipped with an Al monochromatized X-ray source driven at 10 kV and 20 mA from Surface Science Instruments (USA). Samples in the form of powder were compacted within metallic troughs of 4 mm diameter using a press. Next, they were collocated on a ceramic carousel enclosed with a Ni grid to facilitate charge stabilization. Samples to be tested were degassed overnight at 10^{-7} Pa prior to their transfer to the analysis chamber at 10^{-9} Pa. Analyses began by adjusting the angle between the carousel surface and the axis analyzer at 55°, while the flood gun was adjusted at 8 eV. Other parameters such as the full width measured at half maximum (FWHM) of the Au $4f_{7/2}$ peak of a gold standard and pass energy were set at 1.6 and 150 eV, respectively. A survey spectrum was collected first, followed by C 1s, O 1s, N 1s, Cl 2p, and Ru 3p. It is important to mention that a second C 1s spectrum was collected to verify the stability of charge compensation with time. All spectra were treated with the CasaXPS program (Casa Software Ltd, U.K.) to estimate the chemical environment of each sample and the Ru oxidation states using the Ru 3p core level specifically.[36]

2.4. Palm Oil Derivatization. First, 300 mg of palm oil was added to 2 mL of *n*-hexane (C_6H_{14}, >96% from TCI chemicals) and mixed with 1 mL of a 2 M KOH−methanol solution (KOH, 99% from Acros Organics; CH_3OH, 99% from TCI chemicals) to hydrolyze the triglycerides and to release all fatty acids (FAs). The mixture was vortexed for 30 s and then heated at 70 °C for 2 min. Then, the organic phase was retrieved and mixed with 1.8 mL of a 2 M HCl−methanol solution (HCl, 37 v/v% from Carl Roth) to ensure the complete transformation of all FAs into their respective methyl esters (Scheme S1). The new solution was heated at 90 °C for 1 h. Next, the solution was cooled down to room temperature, with the subsequent addition of 1 mL of distilled H_2O. Afterward, the solution was vortexed for 30 s, and the organic layer was extracted and placed in a round flask of 50 mL. To determine the lipidic profile of palm oil, 0.1 mL from the organic phase was mixed with 1.4 mL of *n*-hexane and injected in a gas chromatograph (Varian 3800 equipped with a Stabilwax-DA Restek column) with a flame ionization detector

https://doi.org/10.1021/acs.iecr.2c04498
Ind. Eng. Chem. Res. XXXX, XXX, XXX−XXX

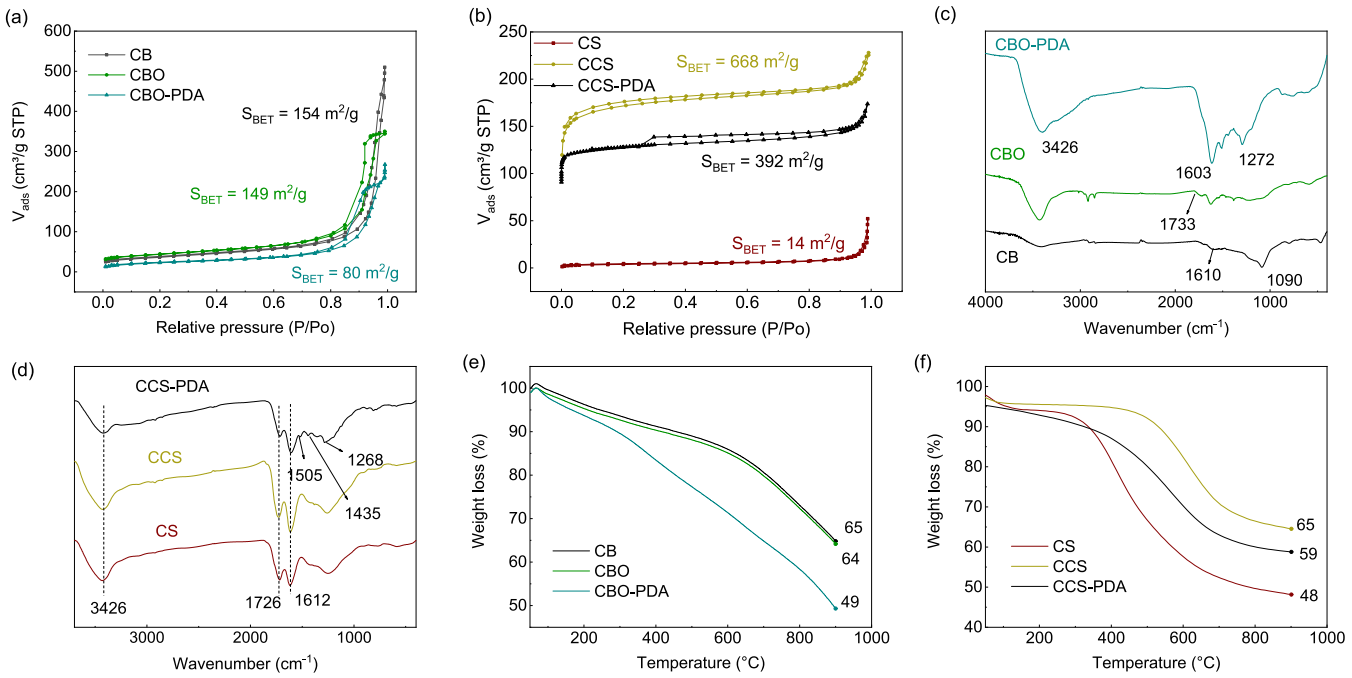

Figure 2. (a) N_2 isotherms of CB, CBO, and CBO-PDA; (b) N_2 isotherms of CS, CCS, and CCS-PDA; (c) FTIR spectra CB, CBO, and CBO-PDA; (d) FTIR spectra of CS, CCS, and CCS-PDA; (e) TGA curves of CB, CBO, and CBO-PDA; and (f) TGA curves of CS, CCS, and CCS-PDA.

(FID) and a database with the main FAs. Finally, the organic phase in the round flask was evaporated in a rotary evaporator (50 °C) to obtain FAMEs as a pasty solid.

2.5. Catalytic Tests. The FAME pasty solid (300 mg of which ~150 mg are UFAs) was incorporated into our biphasic catalytic system composed of 2 mL of ethyl acetate (AcOEt, >99.9%, Carl Roth), 4 mL of acetonitrile (MeCN, >99.98%, Carl Roth), and 8 mL of distilled H_2O. Next, 8 equiv (870 mg) of $NaIO_4$ (sodium metaperiodate, >99% from Sigma-Aldrich), with respect to UFAs, along with 100 mg of either CBO-PDA-Ru(2%) or CCS-PDA-Ru(2%) were introduced in the reactor and submitted to magnetic stirring at room temperature for 24 h. In another series of tests, 4 equiv (291 mg) of NMO (>98%, Alfa Aesar) was combined with 4 equiv of $NaIO_4$ (428 mg) and used in place of 8 equiv of $NaIO_4$ (855 mg) to assess the influence of NMO in the oxidative cleavage reaction. To monitor the catalytic runs, samples (0.1 mL organic phase + 1.4 mL of AcOEt) at different time intervals were injected in a gas chromatograph (Varian 3800) to measure the disappearance of UFAs and the formation of pelargonic acid (PA) and methyl azelate (MA). When the catalytic test ended, 2 mL of AcOEt was added to the aqueous phase, vortexed for 30 s, and extracted to ensure that all PAs and MAs that might have formed an emulsion were recovered. The equations employed to determine conversion and selectivities are explained in the Supporting Information. To perform the recycling tests, the recovered catalysts were first washed with distilled H_2O, preheated at 90 °C, and dried at room temperature overnight. Afterward, the recovered and washed carbon catalysts were reintroduced in a new catalytic system with FAMEs from palm oil to perform a catalytic run again. In this study, five consecutive catalytic runs were carried out to assess the stability of both catalysts.

2.6. Azelaic Acid Isolation. Once the catalytic test ended, the organic layer was separated by means of a syringe. Then, 2 mL of AcOEt was added to the aqueous phase, vortexed for 30 s, and extracted to assure that all MA and PA were recovered. This procedure was repeated 3 times in total. Then, the AcOEt + MA and PA layer was evaporated using a rotary evaporator at 50 °C to obtain the oxidative cleavage products as a paste. The latter was incorporated in 5 mL of the 2 M KOH−MeOH solution to transform all methyl esters into carboxylic acids. The reaction was interrupted after adding 5 mL of distilled H_2O and the subsequent heating at 90 °C for 15 min to dissolve all AA in warm H_2O (only AA is soluble in warm water).[14] The aqueous solution was separated from the organic phase with a syringe and placed in a vessel. Once the aqueous solution cooled down at room temperature, azelaic acid precipitated. The as-obtained product was weighed and dissolved in 3 mL of deuterated chloroform ($CDCl_3$, 99.8% from Euristop) to confirm the extraction of AA by means of nuclear magnetic resonance (NMR) spectroscopy using a Nuclear Magnetic Resonance Bruker Avance II 300 MHz. The machine operates with a probe z-gradient coil OF 5 mm performing 16 scans during each test. The ^1H spectrum was recorded in a spectral window up to 16 ppm using the singlet signal of $CDCl_3$ for zero calibration. The ^1H spectrum was treated with MestReNova software.

3. RESULTS AND DISCUSSION

3.1. Characterized Carbon Materials. The TEM image in Figure 1a shows how CB is arranged as a set of spheres that form nodules. The oxidation treatment with HNO_3 did not cause drastic ruptures of these nodules since CBO in Figure 1b maintained the same morphology that CB. In addition, the mean particle size of CB and CBO was almost the same, 27 and 28 nm, respectively (Table S1). Figure 1c shows how CBO nodules are enveloped by PDA during the self-polymerization of dopamine, causing the increase of average particle size from 28 to 41 nm.

https://doi.org/10.1021/acs.iecr.2c04498
Ind. Eng. Chem. Res. XXXX, XXX, XXX−XXX

As regards carbon nanoparticles, the TEM image in Figure 1d confirms that indeed the hydrothermal carbonization method produced spherical carbon particles with ∼360 nm. Soft calcination reduced the average size of CCS particles down to 221 nm (Figure 1e). The reason for this particle size reduction is related to the CS chemical structure. Normally, CS is composed of many small curved graphitic layers compacted over each other.[37] During the calcination treatment under an air atmosphere, the graphitic layers detached from each other uniformly with the consequent combustion of these carbon moieties, which leads to a uniform particle size reduction of CS.[38] On the other hand, Figure 1f shows how PDA is attached to calcined carbon spheres (CCS), increasing their mean particle size from 221 to 243 nm. In both cases (i.e., CBO-PDA and CCS-PDA), the polymer covered the surfaces of each carbon support, increasing their mean particle size.

Figure 2a shows the N_2 physisorption isotherms of CB, CBO, and CBO-PDA. These carbon materials presented a type 2 isotherm along with a thin-type H3 hysteresis loop characteristic of materials with big mesopores. Due to PDA deposition, the CBO surface area was reduced to 80 m^2/g. Following the same trend, pore volume also diminished from 0.58 to 0.33 cm^3/g because the polymer filled the spaces among the particles. CS also showed a type 2 isotherm bearing a low specific surface area of barely 14 m^2/g. The opposite was observed with CCS (surface area = 668 m^2/g), which displays a type 1 isotherm characteristic of microporous materials (Figure 2b). This finding can be justified by the fact that CS was also submitted to an activation process during the calcination treatment. Although oxygen inside the oven cannot produce a high porosity, it is important to note that CO_2 (formed spontaneously during combustion) can react with carbon on the graphitic layers of CS yielding micropores.[39,40] In addition, the mean pore size of CCS (Table S1) was smaller than the interstitial spaces found during TEM analysis. Therefore, this evidence confirmed that CCS acquired a smaller particle size with a higher surface area compared to CS. As a result of PDA deposition on the CCS surface, most of the micropores were blocked, which in turn caused a drastic decrease in the specific surface area from 668 to 392 m^2/g (Figure 2d). Additionally, the textural properties of both carbon supports suffered significant changes when Ru was deposited on their surfaces (Table S1).

The influence of PDA on the chemical characteristics of both carbon supports was studied through infrared spectroscopy and Boehm's titration. Figure 2c shows peaks at 1610 and 1200 cm^{-1} that belong to ring stretch vibrations in aromatic compounds and lactone groups on CB.[41] Moreover, the intense peak at 1091 cm^{-1} is ascribed to the C−O stretch vibration mode from the phenol bond in alcohols.[41] After the oxidation treatment, a small peak at 1733 cm^{-1} appears in the CBO spectrum, which corresponds to the C═O stretching vibration mode.[42] When PDA was deposited over the CBO surface, the later peak disappeared and new ones were observed at 3426, 1603, and 1272 cm^{-1}. These peaks, which were also detected in the FTIR spectrum of pure PDA (Figure S1), belong to the stretching vibrations in O−H bonds of catechol groups, N−H stretching vibration or aromatic amines, and C−N stretching vibration in the indole ring of the polymer, respectively.[43−45] Thus, these findings confirm the presence of PDA on the CBO surface. The FTIR spectrum of carbon particles (Figure 2d) presents three peaks at 3426, 1726, and 1612 cm^{-1}, which belong to (O−H), carbonyls (C═O), and ring stretching in aromatic compounds.[42] This spectrum confirms that the hydrothermal treatment was successful in producing a carbon support already functionalized with oxygenated groups. The same peaks remained after the calcination treatment (CCS), while in the case of CCS-PDA, three new bands attributed to the N−H stretching (1505 cm^{-1}), N−H scissoring vibration (1435 cm^{-1}), and C−N stretching vibration (1268 cm^{-1}) were detected.[42−46] Thus, CBO and CCS were successfully functionalized with PDA. In addition, no additional peaks were evidenced after Ru impregnation on each carbon support during FTIR analyses.

Table S2 (Boehm's titration results) demonstrates that the oxidation treatment on CB contributed to the increase in the amount of OH groups from 0.06 to 0.43 mmol/g. Conversely, lactones did not change while carboxylic groups were produced on CBO. The addition of PDA increased the amount of OH functionalities even more, up to 0.66 mmol/g. These extra OH groups can be employed for the chelation of Ru during the preparation of the catalyst. Conversely, CS presents the greatest number of oxygenated groups of all samples tested in this research. Thus, hydrothermal carbonization produced spherical carbon particles already functionalized without using hazardous reagents or additional oxidation treatments. CCS maintained the same functional groups but in less amount than CS due to the carbon layers' detachment provoked by the calcination procedure. An important finding was related to the phenol increase (up to 1.23 mmol/g) when PDA was deposited on the CB surface in spite of the total acidity decreasing. Moreover, this number of phenols was large enough to welcome Ru ions to prepare to reach a Ru loading of 4 wt % on the support. Consequently, the synthesis of Ru-carbon catalysts with a nominal content in Ru of 2 wt % was not an issue.[24]

TGA curves (Figure 2e,f) of the two assessed composites show two well-defined stages. The first one corresponds to moisture evaporation trapped in each carbon support. The second stage is related to the thermal decomposition of the carbon structure under an inert atmosphere. CB and CBO presented the same trends, which confirms that the oxidation treatment did not affect at all the carbonaceous structure. Conversely, CS started to decompose at 305 °C, while at 420 °C, the solid lost 20% of its mass. This data was employed to determine at which temperature the calcination treatment should be performed. CCS exhibited better thermal stability since its decomposition started at higher temperatures (470 °C). An increase in weight loss was observed in CBO-PDA and CCS-PDA thermograms, which is attributed to the thermal decomposition of the polymer (Figure S1c). The moisture within the polymer matrix evaporated in a temperature range of 50 °C < T < 250 °C and then the polymer started to decompose up to 900 °C. The difference in the weight loss of unfunctionalized carbon supports and the weight loss of carbon materials with PDA yielded the content of the polymer. Thus, PDA content was 15 wt % on the CBO surface, while CCS possessed 6 wt % on its surface.

The impregnation of Ru was performed on both carbon supports functionalized with polydopamine (CBO-PDA and CCS-PDA). ICP results summarized in Table 1 demonstrated that Ru experimental loadings agree with the nominal value (2 wt %). These results confirm that PDA functional groups were capable of complex Ru ions from the aqueous solution to synthesize the carbon catalyst with the targeted Ru loading.

https://doi.org/10.1021/acs.iecr.2c04498
Ind. Eng. Chem. Res. XXXX, XXX, XXX−XXX

Table 1. Ru Load on Fresh CBO-PDA and CCS-PDA

catalyst	theoretical Ru loading (wt %)[a]	superficial Ru loading (wt %)[b]	experimental Ru loading (wt %)[c]
fresh CBO-PDA-Ru	2.0	2.3	1.9
fresh CCN-PDA-Ru	2.0	2.5	1.8

[a]Theoretical Ru content (2 wt %). [b]Amount of Ru estimated by XPS. [c]Ru content by ICP-AES.

XPS spectra (Figure 3a,b) show peaks at 284.8, 532.8, and 400.0 eV, which correspond to C 1s, O 1s, and N 1s peaks, respectively. The nitrogen peak is attributed to the presence of nitrogen atoms within PDA on CBO and CCN surfaces. Pure PDA was also analyzed by XPS spectroscopy to understand the chemical environment of the polymer (Figure S1). The C 1s spectrum of PDA was fitted into four subpeaks: 284.8 eV (CH−CH), 286.3 eV (C−O−H of catechol groups or primary amines), 288.1 eV (C═O carbonyl groups), and 290.1 eV ($\pi-\pi^*$), which belongs to aromatic structures.[45] Similarly, the N 1s peak was disentangled in three contributions (398.6, 400.0, and 401.8 eV) which can be attributed to imines (═NH−R), secondary amines (R−NH−R), and a primary amine (R−NH_2). Imines and secondary amines are part of the indole ring of PDA, while primary amines are related to unpolymerized moieties of dopamine, which suggest that the polymerization process was not complete.[47] As regards CBO-PDA-Ru(2%) and CCS-PDA-Ru(2%), two peaks at 463.3 and 485.5 eV were observed in both XPS survey spectra (Figure 3a,b), which correspond to Ru $3p_{3/2}$ and Ru $3p_{1/2}$. These peaks were used to discern the oxidation state of Ru on both functionalized carbon supports. C 1s high-resolution spectra of CBO-PDA-Ru(2%) and CCS-PDA-Ru(2%) were deconvoluted to the following contributions (Figure 3c,d): 284.8 eV (C−H), 286.2 eV (C−O/C−N), 287.7 eV (C═O), 288.9 eV (COOH), and a shake-up peak at 291 eV. These species agree with those found in FTIR spectra as well as in the PDA chemical structure. In addition, a doublet at Ru $3d_{5/2}$ = 282.0 and Ru $3d_{3/2}$ = 286.2 eV confirmed the oxidation state of Ru^{III}.[37] Most likely, catechol groups of PDA are complexing Ru ions.

Finally, the Ru 3p doublet was also analyzed (Figure 3e,f) on CBO and CCS functionalized surfaces. As regards CBO-PDA-Ru(2%), three contributions were observed at 463.5 and 467.2 eV, which are assigned to Ru^{III} and a satellite peak of Ru^{III}. On the other hand, CCS-PDA-Ru(2%) presents two peaks at 463.2 and 485.4 eV, which correspond to Ru^{III}. A ligand substitution took place during the impregnation of Ru on CBO-PDA and CCS-PDA surfaces due to no Cl being observed in the spectra. Most likely, Cl was replaced by catechol groups from polydopamine, which led to the formation of a Ru^{III}-catecholate complex.[48,49] Table 2 summarizes the surface chemical composition of the prepared Ru catalysts.

Table 2. Surface Composition (wt %) of Ru-Carbon Catalysts from XPS

catalysts	C 1s (%)	O 1s (%)	N 1s (%)	Ru 3p (%)
CBO-PDA-Ru(2%)	75.7	17.0	5.0	2.3
CCS-PDA-Ru(2%)	69.5	20.5	7.5	2.5

3.2. Catalytic Test Results. Before assessing the catalytic performances of CBO-PDA-Ru(2%) and CCS-PDA-Ru(2%) in the oxidative cleavage of UFAs, the lipidic profile of Ecuadorian palm oil was explored (Table S3). This vegetable oil contains 41% of oleic acid and 9% of linoleic acid. These UFAs represent about half of the total fatty acids composition in palm oil, and both oleic and linoleic acids can be used for the production of AA, as described in Scheme S2. Since

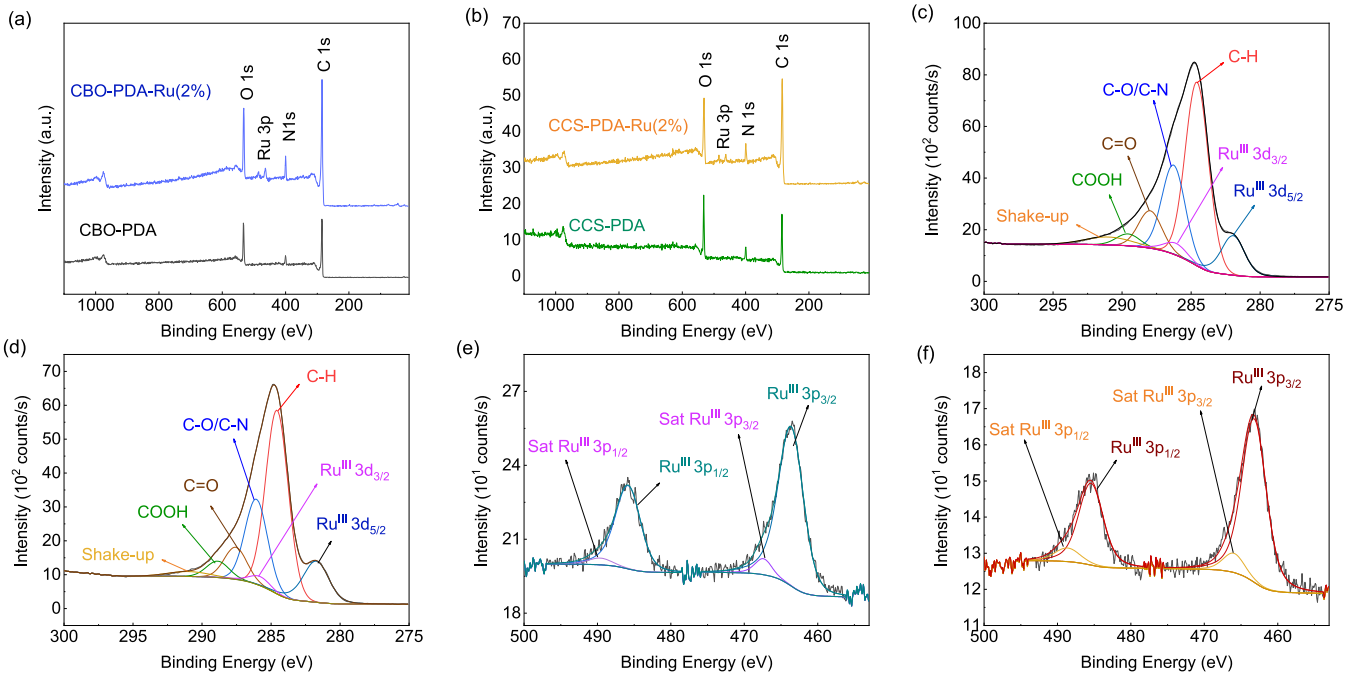

Figure 3. (a) Survey spectra of CBO-PDA and CBO-PDA-Ru(2%); (b) survey spectra of CCS-PDA and CCS-PDA-Ru(2%); and high-resolution XPS spectra of (c) C 1s from CBO-PDA-Ru(2%); (d) C 1s from CCS-PDA-Ru(2%); (e) Ru 3p from CBO-PDA-Ru(2%); and (f) Ru 3p from CCS-PDA-Ru(2%).

https://doi.org/10.1021/acs.iecr.2c04498
Ind. Eng. Chem. Res. XXXX, XXX, XXX−XXX

Scheme 1. Pelargonic Acid and Methyl Azelate Production from Ecuadorian Palm Oil

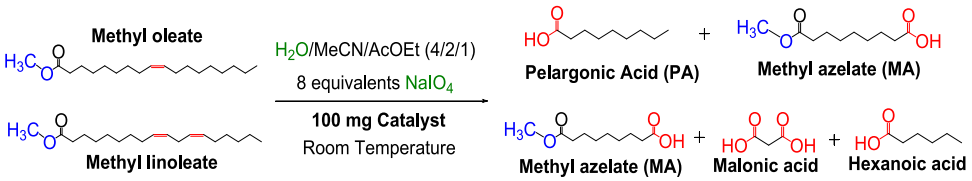

linoleic acid has two unsaturations, the molecule is split into three parts after the scission of its carbon−carbon double bonds. Consequently, three products are obtained: azelaic acid, hexanoic acid, and malonic acid. In this work, we assessed the catalytic behavior of our synthesized Ru catalysts in the production of PA and MA using oleic and linoleic acids within palm oil as raw materials. For this matter, triglycerides inside the palm oil were hydrolyzed to release the mentioned UFAs, as shown in Scheme S1.

Methanol, along with KOH, can break the triglycerides releasing FAs as methyl esters. To ensure a complete esterification of all free FAs, a HCl−MeOH solution was used as well.[50] After fatty acids (saturated and unsaturated ones) transformed into FAMEs, they were incorporated into our biphasic solution formed by H_2O/MeCN/AcOEt (4/2/1). The organic layer (i.e., AcOEt) is used for the dissolution of all FAMEs coming from palm oil, while H_2O is used for the dissolution of the oxidizing agent (i.e., $NaIO_4$), which is essential for the oxidation of Ru^{III}-catecholate complexes on the carbon catalyst surface into $Ru^{VIII}O_4$. MeCN may form complexes with potential leached Ru ions to prevent their volatilization.[14] Thus, methyl oleate and methyl linoleate can be transformed into PA and MA under the conditions stated in Scheme 1 with both synthesized carbon catalysts. It is necessary to mention that the transformation of UFAs into FAMEs is not mandatory for efficient performance in the oxidative cleavage reaction. In fact, our synthesized catalysts can cleave olefinic bonds of UFAs when they form part of triglycerides. The monitoring of the catalytic reaction through FAME peak disappearance in the chromatograms is the main reason why the hydrolysis of triglycerides was carried out.

First, the olefinic bond of oleic acid was cleaved with the carbon supports to verify if the carbon materials (functionalized with PDA or not) may have catalytic activity in this reaction. Table 3 shows that all carbon supports are not active in the oxidative cleavage reaction.

The same procedure was applied with both oxidizing agents (i.e., $NaIO_4$ and NMO) without the solid catalyst. In both cases, the conversions reached were lower than 1%, confirming that the reaction cannot proceed with just the oxidizing agents or the carbon supports. Figure 4a shows the catalytic activity displayed by CBO-PDA-Ru(2%) and CCS-PDA-Ru(2%) in the oxidative cleavage of UFAs within palm oil. These reactions were carried out with 8 equiv of $NaIO_4$ and, as in the case of the catalytic tests with pure oleic acid reported in our previous publication,[24] both catalysts accomplished almost total conversion in 7 h of agitation. CCS-PDA-Ru(2%) showed a greater conversion than CBO-PDA-Ru(2%) at the early stages of the catalytic test. This phenomenon is attributed to the higher surface area of CCS compared to CBO ones. These results demonstrate that other palm oil components (e.g., SFAs or minor components like carotenoids) were not detrimental to the catalyst's performances in the oxidative cleavage reaction. In addition, yields and selectivity of PA were around 78%, while MA yields were around 95%. It is worth mentioning that a 20% surplus is expected with MA since this product can be produced from methyl oleate (41% in palm oil) and methyl linoleate (9% in palm oil). The same trend was also observed with the product distribution in Figure S2. These results confirm that both carbon-PDA-Ru catalysts are as active and selective as in the case of pure oleic acid.[24]

Table 3. Conversion and Yields of PA and MA[a]

carbon material	conv. (%)	PA (%)	MA (%)
CBO	0.5	NA	NA
CCS	0.4	NA	NA
CBO-PDA	0.6	NA	NA
CCS-PDA	0.5	NA	NA
$NaIO_4$[b]	0.5	NA	NA
NMO[c]	0.4	NA	NA

[a]Catalytic tests conducted with 300 mg of palm oil, magnetic stirring, 8 equiv of $NaIO_4$ for 24 h at room temperature, and 100 mg of each carbon support. [b]4 equiv of $NaIO_4$. [c]4 equiv of NMO.

When $NaIO_4$ was substituted by NMO, no conversion was observed since the amine oxide was not capable of oxidizing the Ru^{III} species on the catalyst surface into the $Ru^{VIII}O_4$ active species. NMO can only reoxidize $H_2Ru^{VI}O_4$ species, as shown in Scheme S3. However, the combination of 4 equiv of $NaIO_4$ and 4 equiv of NMO had a synergistic effect on the catalytic rate of the tested carbon materials since conversion was greater than in the case when 8 equiv of $NaIO_4$ (Figure 5a) was employed. It is worth mentioning that the CCS catalyst finished the oxidative cleavage reaction just after 5 h of magnetic stirring.

Hence, the addition of a greener co-oxidant allowed us to improve the performance of both carbon catalysts without using great amounts of a strong oxidizing agent such as $NaIO_4$. As regards the production of PA and MA, Figure 5b shows yields and selectivity of ∼90% ascribed to PA and yields/selectivities around 74% as regards MA. Therefore, the evidence displayed in Figures 4 and 5 confirms that it is possible to perform the valorization of palm oil efficiently with our catalytic system without any concern about interferences from SFAs or other minor components within this vegetable oil.

During the oxidative cleavage tests with pure oleic acid,[24] it was demonstrated that Ru was released in the aqueous phase. To verify this possibility with palm oil, UV−visible monitoring analyses were conducted on the organic phase during catalytic tests with CBO and CCS catalysts. The spectra displayed in Figure S3 confirm that both $Ru^{VIII}O_4$ and $H_2Ru^{VI}O_4$ species have been present in the organic phase since the early stages of the reaction.[51−54] The former species is responsible for triggering the oxidative cleavage of UFAs by means of a pericyclic [3 + 2] reaction yielding a perruthenate intermediate. On the other hand, $H_2Ru^{VI}O_4$ species is the outcome of the perruthenate decomposition. This Ru species

https://doi.org/10.1021/acs.iecr.2c04498
Ind. Eng. Chem. Res. XXXX, XXX, XXX−XXX

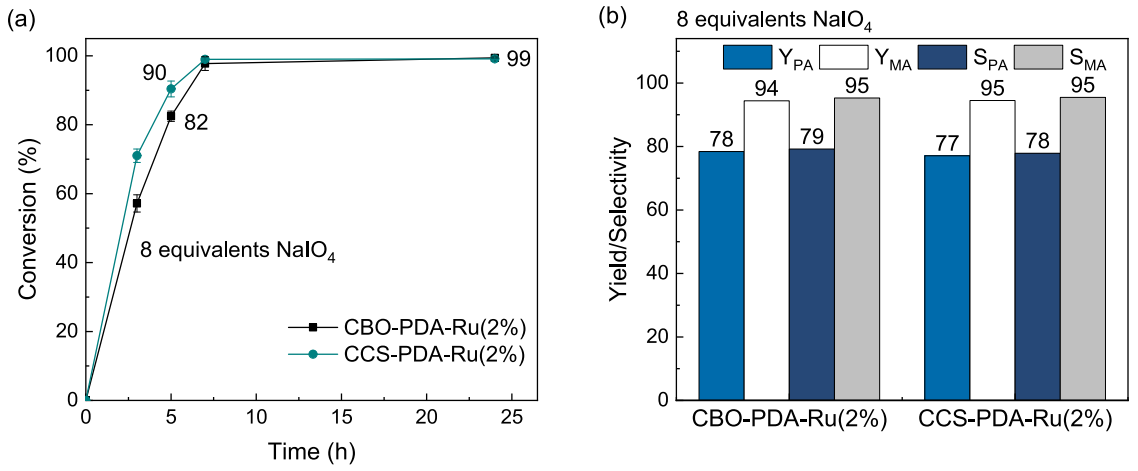

Figure 4. (a) Conversion and (b) yields of PA and AA with of CBO-PDA-Ru(2%) and CCS-PDA-Ru(2%) along with 8 equiv of $NaIO_4$.

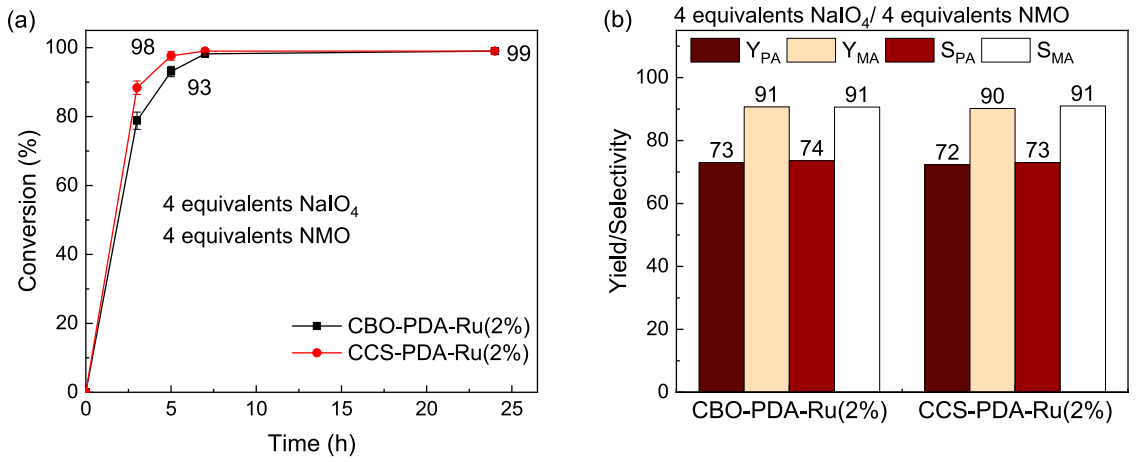

Figure 5. (a) Conversion and (b) yields and selectivities reached with Ru-carbon catalysts using 4 equiv of $NaIO_4$ as an oxidant and 4 equiv of NMO as a co-oxidant.

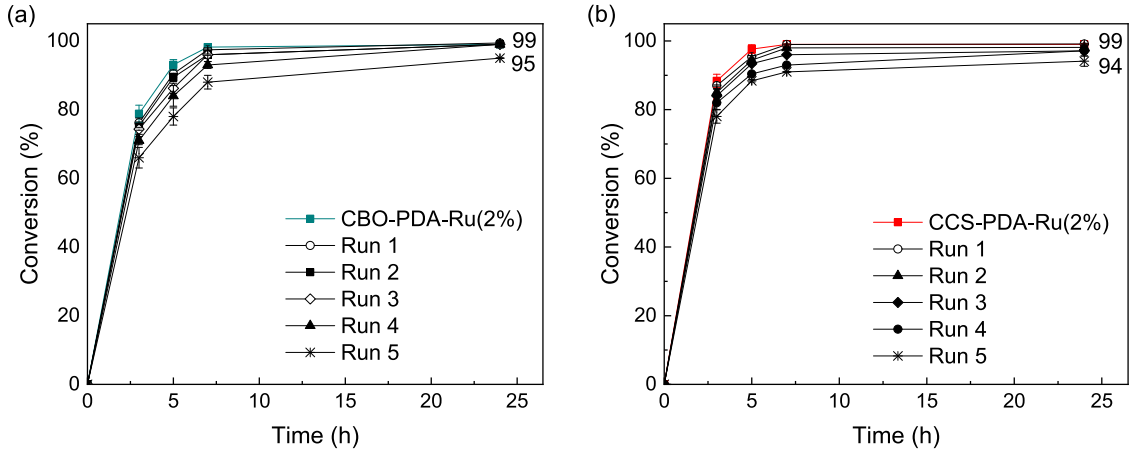

Figure 6. Recycling runs of (a) CBO-PDA-Ru(2%) and (b) CCS-PDA-Ru(2%) using 4 equiv of $NaIO_4$ as an oxidant and 4 equiv of NMO as a co-oxidant.

can be reoxidized to $Ru^{VIII}O_4$ by means of NMO or $NaIO_4$. Moreover, both Ru species disappeared from the organic phase after 24 h of agitation. XPS characterization on spent catalysts in Figure S4 showed the Ru 3p high-resolution spectra displaying two contributions at 462.5 and 463.7 eV which are ascribed to Ru^{III} and Ru^{IV}, respectively. These findings confirm that PDA functional groups on the CBO and CCS surface readsorbed Ru from the reaction medium.

Recycling tests were carried out to check the stability of CBO and CCS catalysts. Figure 6 demonstrates that CBO-PDA-Ru(2%) and CCS-PDA-Ru(2%) attained the same conversion up to five consecutive catalytic tests. Only a slight

https://doi.org/10.1021/acs.iecr.2c04498
Ind. Eng. Chem. Res. XXXX, XXX, XXX−XXX

drop of catalytic activity is noted, likely due to the unavoidable loss of the catalyst when transferring it from one run to the next one.

These results, along with Ru loadings on spent catalysts (Table 4), confirm that PDA adsorbs Ru ions from the liquid phase. In this manner, the same catalytic activity is assured in subsequent catalytic tests.

Table 4. Ru Load on Spent CBO-PDA and CCS-PDA

catalyst	theoretical Ru loading (wt %)[a]	superficial Ru loading (wt %)[b]	experimental Ru loading (wt %)[c]
spent CBO-PDA-Ru(2%)	2.0	2.2	1.8
spent CCS-PDA-Ru(2%)	2.0	2.1	1.7

[a]Theoretical Ru content (2 wt %). [b]Amount of Ru estimated by XPS. [c]Ru content by ICP-AES.

In addition, all of the information gathered in this work suggests that SFAs and other minor components of palm oil did not hinder the interaction of Ru species with UFAs. This is in line with the fact that the catalyst performances with this vegetable oil were similar as in the case with pure oleic acid.[24]

Isolated yields of AA with our two Ru-based functionalized carbon catalysts are reported in Table 5 compared with those reported in the literature. The obtained white product was characterized by NMR spectroscopy (Figure S5), confirming that indeed AA was separated from the liquid phase. These results confirm that AA can be produced from palm oil using our modified carbon catalysts. Moreover, isolated yields reached by our carbon-PDA-Ru catalysts are greater than those reported in the literature such as the works of Rup et al. (78% AA)[14] or Ho and co-workers (79% AA).[16] As regards AA yields when using vegetable oils as raw materials,[17,18] the values reported in the literature are lower than the results achieved with our synthesized carbon catalysts. Therefore, the methodology applied to isolate AA from the rest of the components within the organic phase was efficient since the isolated yields are close to those calculated from GC results. In this way, it is possible to propose a simple process to produce AA from a cheap and abundant feedstock such as palm oil. Scheme 2 recapitulates the main steps required for the production of this dicarboxylic acid without the need to separate UFAs from the vegetable oil.

First, palm oil is submitted to hydrolysis along with the 2 M KOH−methanol solution to release all FAs within the feedstock. During this process, some FAs can be transformed into FAMEs. To standardize the blend, all free FAs from the previous step were transformed into FAMEs using the 2 M HCl−MeOH solution. Next, all FAMEs (which include saturated and unsaturated ones), along with minor components (e.g., carotenoids), are incorporated into the catalytic system (i.e., the biphasic solution of H_2O/MeCN/AcOEt: 4/2/1). The oxidative cleavage reaction takes place for 24 h at room temperature using our Ru-carbon catalysts functionalized with PDA. Although the complete transformation of UFAs into carboxylic and dicarboxylic acids can be accomplished in 5 h using NMO−$NaIO_4$ (4 equiv−4 equiv), the reaction must proceed to assure the total recovery of Ru species from the reaction medium by PDA functional groups. Thus, catalysts maintain >99% conversion for several runs.

Then, the solid catalyst and the aqueous phase should be separated by physical means and recycled into the oxidative cleavage process to reuse the catalyst and avoid losses of Ru (which can also be detrimental to the environment). The organic phase is then treated with the 2 M KOH−MeOH solution to transform all FAMEs into carboxylic acids. Finally, the organic phase is mixed with distilled H_2O at 90 °C to solubilize the azelaic acid in the aqueous phase. After separating water from the organic phase, the aqueous solution is allowed to cool down at room temperature to promote the precipitation of azelaic acid as white crystals. Thus, this proposed and simple methodology can be implemented for the valorization of palm oil in regions where this natural feedstock is abundant and cheap, yielding high-value products such as AA.

4. CONCLUSIONS

Palm oil valorization was possible through the oxidative cleavage of UFAs within the vegetable oil using Ru-carbon catalysts to yield pelargonic and azelaic acids in high yields (~80%). The addition of NMO as a co-oxidizing agent decreased the time required to complete the transformation of UFAs (i.e., oleic and linoleic acids) into the desired oxidative cleavage products by about 30%.

Recycling tests demonstrated that conversions were greater than 95% even after five consecutive catalytic tests, along with high yields toward the oxidative cleavage products. Thus, it was confirmed that SFAs and other minor components (e.g., carotenoids) within palm oil do not interfere in the oxidative cleavage reaction with Ru-carbon catalysts.

UV−visible monitoring tests showed that $Ru^{VIII}O_4$ and $H_2Ru^{VI}O_4$ were in the reaction medium performing the oxidative cleavage reaction in the same way as in the case with pure oleic acid.

To subject a vegetable oil to the oxidative cleavage reaction, it is advisable to conduct a hydrolysis step with a KOH−MeOH solution to break triglycerides and release all FAs. Since, in this step, some FAs can be transformed into FAMEs, esterification is advised to complete the transformation of all FAs into FAMEs.

Table 5. Catalytic Performances of Different Catalysts in the Literature and from This Work

catalyst	substrate	oxidant	solvent	conditions	conv. (%)	yield AA (%)[a]	refs
RuO_4	oleic acid	4 equiv $NaIO_4$	H_2O/MeCN/AcOEt	1 h; UI	>99	78	14
Ru/HAP	methyl oleate	2 equiv $NaIO_4$	1,2 dichloroethane/H_2O	RT; 12 h	16	79	16
VO/TiO_2	seed oil	TBHP (70%)	solvent free	80 °C; 12 h	58	66	17
H_2WO_4	olive oil	10 equiv H_2O_2	solvent free	70 °C; 24 h	>99	71 ± 1	18
CBO-PDA-Ru(2%)	palm oil	4 equiv $NaIO_4$; 4 equiv NMO	H_2O/MeCN/AcOEt	RT; 5 h	>99	81 ± 2	this work
CCN-PDA-Ru(2%)	palm oil	4 equiv $NaIO_4$; 4 equiv NMO	H_2O/MeCN/AcOEt	RT; 5 h	>99	80 ± 3	this work

[a]Isolated yields; UI: ultrasound irradiation; RT: room temperature; TBHP: tert-butyl hydroperoxide; HAP: hydroxyapatite.

https://doi.org/10.1021/acs.iecr.2c04498
Ind. Eng. Chem. Res. XXXX, XXX, XXX−XXX

Scheme 2. Proposed Procedure for Palm Oil Valorization through the Oxidative Cleavage of UFAs for Azelaic Acid Production

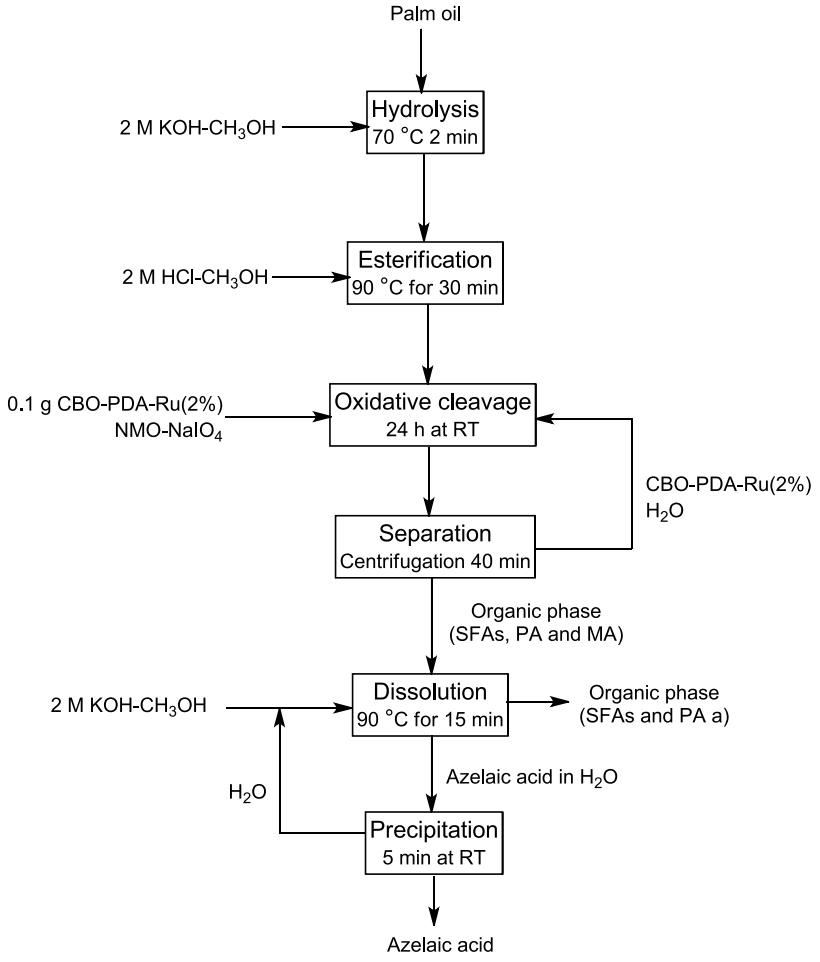

The catalytic test with our Ru-carbon catalysts takes place during 24 of stirring at room temperature to permit catechol groups of PDA to recover Ru ions from the liquid phase and keep the same conversion of our carbon catalysts for several catalytic runs.

Azelaic acid can be separated quite easily from the rest of the blend by adding a 2 M KOH−MeOH solution (to transform monomethyl azelate into azelaic acid) and the addition of distilled H_2O with subsequent heating at 90 °C for 15 min to isolate AA in the aqueous phase.

This new proposed process with our Ru-carbon catalysts opens a novel route to the production of a high-value-added product (i.e., azelaic acid) with medicinal applications from a cheap feedstock such as palm oil.

■ ASSOCIATED CONTENT

Supporting Information

The Supporting Information is available free of charge at https://pubs.acs.org/doi/10.1021/acs.iecr.2c04498.

Additional information related to characterization and catalytic tests (PDF)

■ AUTHOR INFORMATION

Corresponding Author

Sebastián Gámez − *Institute of Condensed Matter and Nanosciences, Université catholique de Louvain, 1348 Louvain-la-Neuve, Belgium;* orcid.org/0000-0002-8850-8604; Email: sebastian.gamez@uclouvain.be

Authors

Ernesto de la Torre − *Department of Extractive Metallurgy, Escuela Politécnica Nacional, Quito 170517, Ecuador*

Eric M. Gaigneaux − *Institute of Condensed Matter and Nanosciences, Université catholique de Louvain, 1348 Louvain-la-Neuve, Belgium;* orcid.org/0000-0003-2239-4306

Complete contact information is available at: https://pubs.acs.org/10.1021/acs.iecr.2c04498

Author Contributions

The present research work is the set of contributions from all mentioned authors. All authors agreed with the final version of this manuscript. S.G. and E.M.G. contributed equally, while E.d.l.T. contributed with supporting and editing throughout the research.

Funding

This research work was possible thanks to the "Coopération au développement" doctoral program granted to S.G. by Université catholique de Louvain, Belgium.

Notes

The authors declare no competing financial interest.

https://doi.org/10.1021/acs.iecr.2c04498
Ind. Eng. Chem. Res. XXXX, XXX, XXX−XXX

■ ACKNOWLEDGMENTS

The authors desire to express their gratitude to the "Université catholique de Louvain" for the scholarship granted to S.G. for the development of the present research work.

■ REFERENCES

(1) Nor Aini, I.; Miskandar, M. S. Utilization of palm oil and palm products in shortenings and margarines. *Eur. J. Lipid. Sci. Technol.* **2007**, *109*, 422−432.
(2) Mamat, H.; Nor Aini, I.; Said, M.; Jamaludin, R. Physicochemical characteristics of palm oil and sunflower oil blends fractionated at different temperatures. *Food Chem.* **2005**, *91*, 731−736.
(3) Lai, O.-M.; Phuah, E.-T.; Lee, Y.-Y.; Basiron, Y. Palm Oil. In *Bailey's Industrial Oil and Fat Products*, Shahidi, F., Ed.; John Wiley & Sons, Ltd: 2020; 1−101.
(4) Laning, S. J. Chemical interesterification of palm, palm kernel and coconut oils. *J. Am. Oil Chem.' Soc.* **1985**, *62*, 400−407.
(5) Anastas, P. T.; Kirchhoff, M. M. Origins, current status, and future challenges of green chemistry. *Acc. Chem. Res.* **2002**, *35*, 686−694.
(6) Enferadi Kerenkan, A.; Béland, A.; Do, T. Chemically catalyzed oxidative cleavage of unsaturated fatty acids and their derivatives into valuable products for industrial applications: a review and perspective. *Catal. Sci. Technol.* **2016**, *6*, 971−987.
(7) Shim, J. O.; Jeong, D. W.; Jang, W. J.; Jeon, K. W.; Kim, S. H.; Jeon, B. H.; Roh, H. S.; Na, J. G.; Oh, Y. K.; Han, S. S.; Ko, C. H. Optimization of unsupported CoMo catalysts for decarboxylation of oleic acid. *Catal. Commun.* **2015**, *67*, 16−20.
(8) Mendes, M. J.; Santos, O. A. A.; Jordão, E.; Silva, A. M. Hydrogenation of oleic acid over ruthenium catalysts. *Appl. Catal., A* **2001**, *217*, 253−262.
(9) Benessere, V.; Cucciolito, M. E.; De Santis, A.; Di Serio, M.; Esposito, R.; Ruffo, F.; Turco, R. Sustainable Process for Production of Azelaic Acid Through Oxidative Cleavage of Oleic Acid. *J. Am. Oil Chem. Soc.* **2015**, *92*, 1701−1707.
(10) Yu, J. S.; Kim, A. K. Effect of combination of taurine and azelaic acid on antimelanogenesis in murine melanoma cells. *J. Biomed. Sci.* **2010**, *17*, S1−S45.
(11) Soutelo-Maria, A.; Dubois, J.-L.; Couturier, J.-L.; Cravotto, G. Oxidative Cleavage of Fatty Acid Derivatives for Monomer Synthesis. *Catalysts* **2018**, *8*, 464.
(12) Zimmermann, F.; Meux, E.; Mieloszynski, J. L.; Lecuire, J. M.; Oget, N. Ruthenium catalysed oxidation without CCl_4 of oleic acid, other monoenic fatty acids and alkenes. *Tetrahedron Lett.* **2005**, *46*, 3201−3203.
(13) Foglia, T. A.; Barr, P. A.; Malloy, A. J.; Costanzo, M. J. Oxidation of unsaturated fatty acids with ruthenium and osmium tetroxide. *J. Am. Oil Chem. Soc.* **1977**, *54*, A870−A872.
(14) Rup, S.; Zimmermann, F.; Meux, E.; Schneider, M.; Sindt, M.; Oget, N. The ultrasound-assisted oxidative scission of monoenic fatty acids by ruthenium tetroxide catalysis: Influence of the mixture of solvents. *Ultrason. Sonochem.* **2009**, *16*, 266−272.
(15) Noureddini, H.; Kanabur, M. Liquid-phase catalytic oxidation of unsaturated fatty acids. *J. Am. Oil Chem. Soc.* **1999**, *76*, 305−312.
(16) Ho, C. M.; Yu, W. Y.; Che, C. M. Ruthenium nanoparticles supported on hydroxyapatite as an efficient and recyclable catalyst for cis-dihydroxylation and oxidative cleavage of alkenes. *Angew. Chem., Int. Ed.* **2004**, *43*, 3303−3307.
(17) Upadhyay, R.; Rana, R.; Sood, A.; Singh, V.; Kumar, R.; Srivastava, V. C.; Maurya, S. K. Heterogeneous vanadium-catalyzed oxidative cleavage of olefins for sustainable synthesis of carboxylic acids. *Chem. Commun.* **2021**, *57*, 5430−5433.
(18) Melchiorre, M.; Benessere, V.; Cucciolito, M. E.; Melchiorre, C.; Ruffo, F.; Esposito, R. Direct and Solvent-Free Oxidative Cleavage of Double Bonds in High-Oleic Vegetable Oils. *ChemistrySelect* **2020**, *5*, 1396−1400.
(19) Studebaker, M. L.; Rinehart, R. W. Infrared studies of oxygen-containing groups on the surface of carbon black. *Rubber Chem. Technol.* **1972**, *45*, 106−116.
(20) Neeft, J. P. A.; Makkee, M.; Moulijn, J. A. Catalytic oxidation of carbon black - I. Activity of catalysts and classification of oxidation profiles. *Fuel* **1998**, *77*, 111−119.
(21) Baccile, N.; Antoniettia, M.; Titirici, M. Hydrothermal carbon from biomass: a comparison of the local structure from poly- to monosaccharides and pentoses/hexoses. *Green Chem.* **2008**, *10*, 1204−1212.
(22) Kubo, S.; White, R. J.; Yoshizawa, N.; Antonietti, M.; Titirici, M. M. Ordered carbohydrate-derived porous carbons. *Chem. Mater.* **2011**, *23*, 4882−4885.
(23) Sevilla, M.; Fuertes, A. B. The production of carbon materials by hydrothermal carbonization of cellulose. *Carbon* **2009**, *47*, 2281−2289.
(24) Gámez, S.; de la Torre, E.; Gaigneaux, E. M. Carbon black-polydopamine-ruthenium composite as a recyclable boomerang catalyst for the oxidative cleavage of oleic acid. *Chem. Eng. J.* **2022**, *427*, No. 131820.
(25) Ye, Q.; Zhou, F.; Liu, W. Bioinspired catecholic chemistry for surface modification. *Chem. Soc. Rev.* **2011**, *40*, 4244−4258.
(26) Lee, H.; Dellatore, S. M.; Miller, W. M.; Messersmith, P. B. Mussel-inspired surface chemistry for multifunctional coatings. *Science* **2007**, *318*, 426−430.
(27) Liu, Y.; Ai, K.; Lu, L. Polydopamine and Its Derivative Materials: Synthesis and Promising Applications in Energy, Environmental, and Biomedical Fields. *Chem. Rev.* **2014**, *114*, 5057−5115.
(28) Du, L.; Liao, R.; Zhang, H.; Qu, X.; Hu, X. Redox-activity of polydopamine for ultrafast preparation of self-healing and adhesive hydrogels. *Colloids Surf., B* **2022**, *214*, No. 112469.
(29) Liu, H.; Qu, X.; Tan, H.; Song, J.; Lei, M.; Kim, E.; Payne, G. F.; Liu, C. Role of polydopamine's redox-activity on its pro-oxidant, radical-scavenging, and antimicrobial activities. *Acta Biomaterialia* **2019**, *88*, 181−196.
(30) Barclay, T. G.; Hegab, H. M.; Clarke, S. R.; Ginic-Markovic, M. Versatile Surface Modification Using Polydopamine and Related Polycatecholamines: Chemistry, Structure, and Applications. *Adv. Mater. Interfaces* **2017**, *4*, No. 1601192.
(31) Jonsson, S. Y.; Färnegårdh, K.; Bäckvall, J. E. Osmium-Catalyzed Asymmetric Dihydroxylation of Olefins by H_2O_2 Using a Biomimetic Flavin-Based Coupled Catalytic System. *J. Am. Chem. Soc.* **2001**, *123*, 1365−1371.
(32) Ottenbacher, R. V.; Talsi, E. P.; Bryliakov, K. P. Recent advances in catalytic asymmetric dihydroxylation of olefins. *Russ. Chem. Rev.* **2019**, *88*, 1094−1103.
(33) Rouquerol, F.; Luciani, L.; Llewellyn, P.; Denoyel, R.; Rouquerol, J. Texture des matériaux pulvérulents ou poreux. *Techniques d'analyse* **2003**, 1−24.
(34) Goertzen, S. L.; Thériault, K. D.; Oickle, A. M.; Tarasuk, A. C.; Andreas, H. A. Standardization of the Boehm titration. Part I. CO_2 expulsion and endpoint determination. *Carbon* **2010**, *48*, 1252−1261.
(35) Chen, J. P.; Wu, S. Acid/Base-Treated Activated Carbons: Characterization of Functional Groups and Metal Adsorptive Properties. *Langmuir* **2004**, *20*, 2233−2242.
(36) Morgan, D. J. Resolving ruthenium: XPS studies of common ruthenium materials. *Surf. Interface Anal.* **2015**, *47*, 1072−1079.
(37) Jin, Y. Z.; Kim, Y. J.; Gao, C.; Zhu, Y. Q.; Huczko, A.; Endo, M.; Kroto, H. W. High temperature annealing effects on carbon spheres and their applications as anode materials in Li-ion secondary battery. *Carbon* **2006**, *44*, 724−729.
(38) Joula, M. H.; Farbod, M. Synthesis of uniform and size-controllable carbon nanospheres by a simple hydrothermal method and fabrication of carbon nanosphere super-hydrophobic surface. *Appl. Surf. Sci.* **2015**, *347*, 535−540.
(39) Guo, J.; Lua, A. C. Microporous Activated Carbons Prepared from Palm Shell by Thermal Activation and Their Application to Sulfur Dioxide Adsorption. *J. Colloid Interface Sci.* **2002**, *251*, 242−247.

https://doi.org/10.1021/acs.iecr.2c04498
Ind. Eng. Chem. Res. XXXX, XXX, XXX−XXX

(40) Gómez-Serrano, V.; Cuerda-Correa, E. M.; Carmen Fernández-González, M.; Alexandre-Franco, M. F.; Macías-García, A. Preparation of activated carbons from walnut wood: a study of microporosity and fractal dimension. *Smart Mater. Struct.* **2005**, *14*, 363−368.
(41) Shurvell, H. F. Spectra− Structure Correlations in the Mid- and Far-Infrared. In *Handbook of Vibrational Spectroscopy*, Chalmers, J. M.; Griffiths, P. R., Eds.; 2006; pp 1783−1816.
(42) Gu, R.; Xu, W. Z.; Charpentier, P. A. Synthesis of polydopamine-coated graphene−polymer nanocomposites via RAFT polymerization. *J. Polym. Sci. Part A: Polym. Chem.* **2013**, *51*, 3941−3949.
(43) Gu, H.; Xu, X.; Dong, M.; Xie, P.; Shao, Q.; Fan, R.; Lu, C.; Wu, S.; Wei, R.; Guo, Z. Carbon nanospheres induced high negative permittivity in nanosilver-polydopamine metacomposites. *Carbon* **2019**, *147*, 550−558.
(44) Wei, Q.; Zhang, F.; Li, J.; Li, B.; Zhao, C. Oxidant-induced dopaminepolymerization for multifunctional coatings. *Polym. Chem.* **2010**, *1*, 1430−1433.
(45) Yu, Y.; Shapter, J. G.; Popelka-Filcoff, R.; Bennett, J. W.; Ellis, A. V. Copper removal using bio-inspired polydopamine coated natural zeolites. *J. Hazard. Mater.* **2014**, *273*, 174−182.
(46) Ball, V. Polydopamine films and particles with catalytic activity. *Catal. Today* **2018**, *301*, 196−203.
(47) Cai, J.; Chen, T.; Cui, L.; Jia, Q.; Liu, M.; Zheng, R.; Yan, G.; Wei, D.; Liu, J. A three-dimensional and porous bi-nanospheres electrocatalytic system constructed by in situ generation of Ru nanoclusters inside and outside polydopamine nanoparticles for highly efficient hydrogen evolution reaction. *Int. J. Hydrogen Energy* **2020**, *45*, 6592−6603.
(48) Öhrström, L.; Michaud-Soret, I. Fe - Catecholate and Fe - Oxalate Vibrations and Isotopic Substitution Shifts from DFT Quantum Chemistry. *J. Phys. Chem. A* **1999**, *103*, 256−264.
(49) Bhattacharya, S.; Ghosh, P.; Chakravorty, A. Ruthenium Tris Chelates with O,S-Siderophores: Synthesis, Oxidation State, and Electronic Structure. *Inorg. Chem.* **1985**, *24*, 3224−3230.
(50) Salimon, J.; Omar, T. A.; Salih, N. Comparison of Two Derivatization Methods for the Analysis of Fatty Acids and Trans Fatty Acids in Bakery Products Using Gas Chromatography. *Sci. World J.* **2014**, *2014*, 1−10.
(51) Boelrijk, A. E. M.; Reedijk, J. Oxidation of methyl- and octyl-αa-d-glucopyranoside, catalysed by high-valent ruthenium species; RuO_4, RuO_4^- and RuO_4^{2-}. *J. Mol. Catal.* **1994**, *89*, 63−76.
(52) Banerjee, D.; Sinharoy, P.; Kaushik, C. P.; Dubey, V. P.; Manohar, S. Studies on volatilization behavior of RuO_4 from nitric acid medium. *Radiochim. Acta* **2020**, *108*, 779−784.
(53) Zerk, T. J.; Moore, P. W.; Harbort, J. S.; Chow, S.; Byrne, L.; Koutsantonis, G. A.; Harmer, J. R.; Martínez, M.; Williams, C. M.; Bernhardt, P. V. Elucidating the mechanism of the Ley-Griffith (TPAP) alcohol oxidation. *Chem. Sci.* **2017**, *8*, 8435−8442.
(54) Chen, J.-Y.; Hsieh, Y.-C.; Wang, L.-Y.; Wu, P.-W. Electroless Deposition of Ru Films Via an Oxidative-Reductive Mechanism. *J. Electrochem. Soc.* **2011**, *158*, D463.

https://doi.org/10.1021/acs.iecr.2c04498
Ind. Eng. Chem. Res. XXXX, XXX, XXX−XXX